A mononuclear Mn^{III}/'bis-tris' complex and its conversion to a mixed-valence $Mn^{II/III}_5$ cluster†

Theocharis C. Stamatatos, Khalil A. Abboud and George Christou*

Received 24th June 2008, Accepted 29th August 2008
First published as an Advance Article on the web 23rd October 2008
DOI: 10.1039/b810701g

The use of the anion of 2,2-bis(hydroxymethyl)-2,2′,2″-nitrilotriethanol ('bis-tris' or LH_5) as a chelate in Mn cluster chemistry is reported, and two products $[Mn(N_3)(LH_3)]$ (**1**) and $[Mn_5(LH_2)_3(LH_5)(MeOH)_{2.5}]Cl_4$ (**2**) are described. The reaction of $Mn(ClO_4)_2{\cdot}6H_2O$ and NaN_3 with LH_5 and NEt_3 in a 1 : 1 : 1 : 2 molar ratio in DMF gave complex **1**. The reaction of **1**, NEt_3 and $MnCl_2{\cdot}4H_2O$ in a 2 : 2 : 1 ratio in MeOH gave the pentanulear complex **2**. Complex **1** contains a distorted-octahedral Mn^{III} atom exhibiting a Jahn–Teller axial elongation. Complex **2** has a mixed-valence $Mn^{II}_2Mn^{III}_3$ trigonal bipyramidal Mn_5 topology, with the apical positions of the $[Mn_5(\mu\text{-}OR)_7]^{6+}$ core occupied by the Mn^{II} atoms. Variable-temperature, solid-state dc and ac magnetization studies are reported for **1** and **2** in the 1.8–300 K range. The data for **1** are as expected for a high-spin d^4 Mn^{III} complex with $S = 2$; at low temperature, the effects of zero-field splitting (ZFS) and intermolecular antiferromagnetic interactions *via* OH···O hydrogen bonds become evident. Fitting of magnetization *vs.* field (H) and temperature (T) data by matrix diagonalization gave $S = 2$, $D = -3.25$ cm^{-1} and $|E| = 0.32$ cm^{-1}, with g fixed at 2.00, where D and E are the axial and rhombic ZFS parameters, respectively. The analogous fit for **2** gave $S = 3$ and $D = -0.68$ cm^{-1}. The combined results demonstrate the usefulness of 'bis-tris' as a new poly-alkoxide chelate for the synthesis of new Mn complexes.

Introduction

There continues to be great interest in the synthesis and study of polynuclear 3d transition metal complexes, not least for their intrinsic architectural beauty and aesthetically pleasing structures.[1] Other reasons for this interest are varied, and for manganese it derives from their relevance to two fields. First, the ability of Mn to exist in three oxidation states (II–IV) under normal conditions has resulted in it being at the active sites of several redox enzymes, such as the water-oxidizing complex (WOC) of photosystem II in green plants and cyanobacteria.[2] Second, polynuclear Mn compounds containing Mn^{III} have been found to often have large, and sometimes abnormally large, ground-state spin values (S). When combined with a large and negative magnetoanisotropy, this has led to some of these species being able to function as single-molecule magnets (SMMs).[3] These are individual molecules that behave as magnets below a certain ("blocking") temperature.[4] Thus, they represent a molecular, 'bottom-up' approach to nanomagnetism.[5]

As a result of the above, we have explored and successfully developed over the years many synthetic routes to new polynuclear Mn complexes,[5,6] with nuclearities currently up to 84.[7] These procedures have included comproportionation reactions of simple starting materials,[8] aggregation of clusters of smaller nuclearity,[9] fragmentation of higher nuclearity clusters,[10] reductive aggregation or fragmentation of preformed clusters,[11] electrochemical oxidation,[12] disproportionation,[13] and ligand substitution of preformed species,[14] among others. As part of this work, we[5,15] and others[16] have also explored a wide variety of potentially chelating and/or bridging ligands that might foster formation of high nuclearity products. Two families of such ligands are the dipodal and tripodal alcohols, which have proved to be extremely versatile chelating and bridging groups that have yielded a number of 3d metal clusters with various structural motifs, large S values, and SMM behaviour.[17] Two examples of such organic species are N-methyldiethanolamine ($mdaH_2$) and 1,1,1-tris(hydroxymethyl)ethane ($thmeH_3$), shown in Scheme 1. As an extension to this productive use of $mdaH_2$ and $thmeH_3$, we have explored the products that might result from the fusion of these two groups into a pentol ligand, namely 2,2-bis(hydroxymethyl)-2,2′,2″-nitrilotriethanol ('bis-tris', hereafter LH_5) shown in Scheme 1.

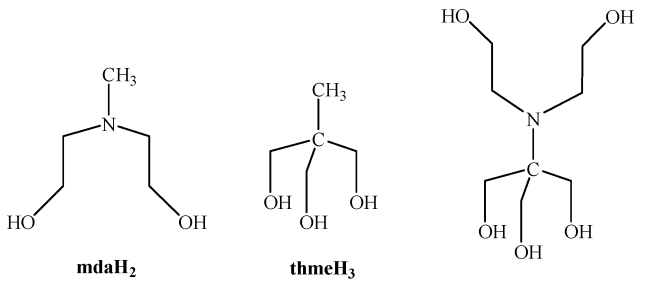

Scheme 1

Department of Chemistry, University of Florida, Gainesville, Florida, 32611-7200, USA. E-mail: christou@chem.ufl.edu; Fax: +1 352-392-6737; Tel: +1 352-392-8314

† Electronic supplementary information (ESI) available: The molecular structure of the cation of **2b**, selected bond distances and angles for **2b**, and BVS calculations for Mn atoms in **2b**. CCDC reference numbers 666391 and 666390 for **1**·½Et_2O and **2**·4MeOH, respectively. For ESI and crystallographic data in CIF or other electronic format see DOI: 10.1039/b810701g

'Bis-tris' (LH_5) is often employed as an aqueous buffer solution for biological materials, and has also been occasionally used in inorganic chemistry for the synthesis of mononuclear Co, Ni, Cu and Zn complexes; these contain neutral LH_5 groups bound through their N and four of the five protonated O atoms.[18] In 3d metal cluster chemistry, the only reported examples are the tetra- and pentanuclear cobalt complexes, $[Co^{III}_4Na^{I}_2(LH)_2(LH_2)_2(MeOH)_4]$ and $[Co^{II}_4Co^{III}(LH)_2(LH_2)_2]$, where the triply- ($LH_2^{3-}$) and quadruply-deprotonated (LH^{4-}) groups act as N,O,O,O,O-chelates to a Co^{III} atom, and link with their deprotonated arms to neighbouring metal atoms.[19]

The fusion of $mdaH_2$ and $thmeH_3$ within LH_5 suggested that the latter would likely give Mn cluster products distinctly different from those obtained with $mdaH_2$ and $thmeH_3$ alone. In the present work, we have explored the reactions between LH_5 and various non-carboxylate Mn starting materials under basic conditions. We shall describe how this study has led to a mononuclear Mn^{III} complex containing a doubly-deprotonated (LH_3^{2-}) N,O,O,O,O chelate, and that this complex is an excellent 'stepping-stone' to a new mixed-valence $Mn^{II}_2Mn^{III}_3$ cluster containing both LH_2^{3-} and LH_3^{2-} bridging groups. The syntheses, structures, and magnetochemical characterization of these complexes are reported herein.

Experimental

Syntheses

All manipulations were performed under aerobic conditions using chemicals and solvents as received, unless otherwise stated. $(NEt_4)_2[MnCl_5]$ was prepared as described elsewhere.[20] ***WARNING**: Azide and perchlorate salts are potentially explosive; such compounds should be synthesized and used in small quantities, and treated with utmost care at all times.*

$[Mn(N_3)(LH_3)]$ (1). To a stirred solution of LH_5 (0.42 g, 2.0 mmol) and NEt_3 (0.56 mL, 4.0 mmol) in DMF (20 mL) was added solid $Mn(ClO_4)_2{\cdot}6H_2O$ (0.72 g, 2.0 mmol). The resulting brown solution was stirred for 1 h, during which time solid NaN_3 (0.13 g, 2.0 mmol) was added in small portions. The solution was stirred for a further 30 min, filtered, and the filtrate layered with Et_2O (40 mL). After 4 days, red crystals of $\mathbf{1}{\cdot}\frac{1}{2}Et_2O$ were collected by filtration, washed with Et_2O (2 × 5 mL), and dried under vacuum over silica gel; the yield was ~70%. The dried solid analysed as solvent-free. Found: C, 36.20; H, 3.55; N, 16.45%. Calcd for $C_8H_{17}MnN_4O_5$: C, 36.10; H, 3.46; N, 16.54%. IR (KBr, cm^{-1}): 3332mb, 2860m, 2551mb, 2069vs, 1477m, 1371m, 1334s, 1243w, 1146m, 1103m, 1059vs, 1017s, 892m, 752m, 717w, 677m, 643w, 579m, 545s, 478m, 410m.

$\{[Mn_5(LH_2)_3(LH_5)(MeOH)_3]Cl_4\}{\cdot}\{[Mn_5(LH_2)_3(LH_5)(MeOH)_2Cl]Cl_3\}$ (2).

Method A. To a stirred, red solution of complex **1** (0.60 g, 2.0 mmol) in MeOH (40 mL) was added NEt_3 (0.28 mL, 2.0 mmol). The resulting dark red solution was stirred for 20 min, during which time solid $MnCl_2{\cdot}4H_2O$ (0.20 g, 1.00 mmol) was added in portions. The solution was stirred for a further 5 min, filtered, and the filtrate left undisturbed to concentrate slowly by evaporation. After 5 d, red crystals of **2**·4MeOH were collected by filtration, washed with cold MeOH (2 × 3 mL) and Et_2O (2 × 5 mL), and dried under vacuum over silica gel; the yield was ~50%. The dried solid analysed as solvent-free using an average formula of $[Mn_5(LH_2)_3(LH_5)(MeOH)_{2.5}]Cl_4$. Found: C, 31.40; H, 5.95; N, 4.11%. Calcd for $C_{34.5}H_{77}Mn_5N_4O_{22.5}Cl_4$: C, 31.29; H, 5.86; N, 4.23%. IR (KBr, cm^{-1}): 3365sb, 2872mb, 1633m, 1469m, 1379m, 1312w, 1256w, 1106m, 1044s, 917m, 893m, 722w, 681m, 623s, 553m, 496w.

Method B. To a stirred, red solution of complex **1** (0.60 g, 2.0 mmol) in MeOH (40 mL) was added NEt_4OH (0.30 g, 2.0 mmol). The resulting dark red solution was stirred for 30 min, during which time solid $(NEt_4)_2[MnCl_5]$ (0.49 g, 1.0 mmol) was added in portions. The solution was stirred for a further 5 min, filtered, and the filtrate left undisturbed to concentrate slowly by evaporation. After 8 d, red crystals were collected by filtration, washed with cold MeOH (2 × 3 mL) and Et_2O (2 × 5 mL), and dried under vacuum over silica gel; the yield was ~35%. The identity of the product was confirmed by elemental analysis (Found: C, 31.47; H, 5.83; N, 4.01%. Calcd for $C_{34.5}H_{77}Mn_5N_4O_{22.5}Cl_4$: C, 31.29; H, 5.86; N, 4.23%), and IR spectroscopic comparison with material from method A.

Method C. To a stirred solution of LH_5 (0.42 g, 2.0 mmol) and NEt_3 (0.64 mL, 6.0 mmol) in MeOH (50 mL) was added solid $MnCl_2{\cdot}4H_2O$ (0.40 g, 2.0 mmol). The resulting dark red solution was stirred for 1 h, filtered, and the filtrate left undisturbed to concentrate slowly by evaporation. After 4 d, red crystals were collected by filtration, washed with cold MeOH (2 × 3 mL) and Et_2O (2 × 5 mL), and dried under vacuum over silica gel; the yield was ~75%. The identity of the product was confirmed by elemental analysis ($[Mn_5(LH_2)_3(LH_5)(MeOH)_{2.5}]Cl_4{\cdot}2H_2O$; Found: C, 30.35; H, 6.21; N, 4.19%. Calcd for $C_{34.5}H_{81}Mn_5N_4O_{24.5}Cl_4$: C, 30.46; H, 6.00; N, 4.12%), and IR spectroscopic comparison with material from method A.

X-Ray crystallography and solution of structure

Data were collected on a Siemens SMART PLATFORM equipped with a CCD area detector and a graphite monochromator utilizing Mo-Kα radiation. Suitable crystals of $\mathbf{1}{\cdot}\frac{1}{2}Et_2O$, and **2**·4MeOH were attached to glass fibres using silicone grease and transferred to a goniostat where they were cooled to 173 K for data collection. An initial search of reciprocal space revealed a triclinic cell for both compounds; the choice of space group $P\bar{1}$ was confirmed by the subsequent solution and refinement of the structures. Cell parameters were refined using up to 8192 reflections. A full sphere of data (1850 frames) was collected using the ω-scan method (0.3° frame width). The first 50 frames were remeasured at the end of data collection to monitor instrument and crystal stability (maximum correction on I was < 1%). Absorption corrections by integration were applied based on measured indexed crystal faces. The structures were solved by direct methods in *SHELXTL6*,[21] and refined on F^2 using full-matrix least-squares. The non-H atoms were treated anisotropically, whereas the H atoms were placed in calculated, ideal positions and refined as riding on their respective C atoms. Unit cell parameters and structure solution and refinement data are listed in Table 1.

For $\mathbf{1}{\cdot}\frac{1}{2}Et_2O$, the asymmetric unit consists of the Mn molecule, and half of a Et_2O molecule of crystallization disordered about an inversion centre. The latter could not be modeled properly, thus the program SQUEEZE,[22] a part of the PLATON package

Table 1 Crystallographic data for **1**·½Et$_2$O and **2**·4MeOH

Formula[a]	$C_{10}H_{22}MnN_4O_{5.5}$	$C_{73}H_{170}Mn_{10}N_8O_{49}Cl_8$
M/g mol^{-1} [a]	341.25	2777.20
Crystal system	Triclinic	Triclinic
Space group	$P\bar{1}$	$P\bar{1}$
a/Å	7.8789(7)	13.0460(7)
b/Å	9.3663(8)	14.7764(7)
c/Å	9.9722(8)	32.4347(16)
α/°	92.000(2)	90.395(1)
β/°	93.201(2)	101.172(1)
γ/°	100.783(2)	110.509(1)
U/Å^3	721.02(11)	5726.2(5)
Z	1	2
T/K	173(2)	173(2)
λ/Å[b]	0.71073	0.71073
ρ_{calc}/g cm^{-3}	1.572	1.621
μ/mm^{-1}	0.945	1.340
Measd/independent	4947/3230	36 154/25 053
(R_{int}) reflns	(0.0456)	(0.1016)
Obsd reflns [$I > 2\sigma(I)$]	2492	16 199
R_1[c,d]	0.0332	0.0648
wR_2[e]	0.0724	0.1584

[a] Including solvent molecules. [b] Graphite monochromator. [c] $I > 2\sigma(I)$. [d] $R_1 = \sum(||F_o| - |F_c||)/\sum|F_o|$. [e] $wR_2 = [\sum[w(F_o^2 - F_c^2)^2]/\sum[w(F_o^2)^2]]^{1/2}$, $w = 1/[\sigma^2(F_o^2) + [(ap)^2 + bp]$, where $p = [\max(F_o^2, 0) + 2F_c^2]/3$.

of crystallographic software, was used to calculate the solvent disorder area and remove its contribution to the overall intensity data. A total of 175 parameters were included in the structure refinement using 2492 reflections with $I > 2\sigma(I)$.

For **2**·4MeOH, the asymmetric unit consists of two Mn_5 clusters, differing only in that one has a terminally-bound MeOH group on Mn3 while the other has a terminally-bound Cl^- ion at this position (Mn8); everything else is the same. There are also seven Cl^- anions and four MeOH molecules of crystallization in the asymmetric unit. One Mn_5 cluster exhibited some disorder problems: The OH groups on C15 (O9) and C30 (O23) are disordered about two sites with 50:50% occupancies. There is also disorder at the bound MeOH groups (O11 and O12) and nearby lattice MeOH groups (O47 and O46) with which they are hydrogen bonding (O11···O47 = 2.700(6) Å, O12···O46 = 2.731(6) Å). There is also extensive hydrogen bonding between the Cl^- anions and OH groups of LH_2^{3-} and LH_3^{2-} chelates, with O···Cl distances all in the 3.0–3.1 Å range, or slightly greater. A total of 1449 parameters were included in the structure refinement using 25 053 reflections with $I > 2\sigma(I)$.

CCDC reference numbers 666391 and 666390 for **1**·½Et$_2$O and **2**·4MeOH, respectively. For crystallographic data in CIF or other electronic format see DOI: 10.1039/b810701g

Other studies

Infrared spectra were recorded in the solid state (KBr pellets) in the 400–4000 cm^{-1} range with a Nicolet Nexus 670 FTIR spectrometer. Elemental analyses (C, H, and N) were performed by the in-house facilities of the University of Florida Chemistry Department. Variable-temperature dc and ac magnetic susceptibility data were collected using a Quantum Design MPMS-XL SQUID susceptometer equipped with a 7 T magnet and operating in the 1.8–300 K range. Samples were embedded in solid icosane to prevent torquing. Magnetization *vs.* field and temperature data were fit using the program MAGNET.[23a] Pascal's constants were used to estimate the diamagnetic corrections, which were subtracted from the experimental susceptibilities to give the molar paramagnetic susceptibilities (χ_M). The values of the diamagnetic susceptibilities for complexes **1** and **2** were calculated as -142.9×10^{-6} cm^3 mol^{-1} for the former and -678.45×10^{-6} cm^3 mol^{-1} for the latter.[23b]

Results and discussion

Syntheses

Most synthetic procedures to polynuclear Mn clusters rely on the reaction of either the triangular $[Mn_3O(O_2CR)_6L_3]^{0,+}$ complexes or simple Mn^{II} salts with a potentially chelating ligand. In particular, thmeH_3 and mdaH_2 have given a number of carboxylate-containing products such as the disk-like $[Mn_9O_7(O_2CMe)_{11}(thme)(py)_3(H_2O)_2]$[24] and a family of Mn_x/thme^{3-} (x = 6–12) rod-like clusters,[25] as well as the loop-like $[Mn_{12}(O_2CMe)_{14}(mda)_8]$ and a $[Mn_4(O_2CPh)_4(mda)_2(mdaH)_2]$ cage.[26] However, in the absence of carboxylate groups, the only structurally-characterised products have been the $[Mn_2(thmeH)_2(bpy)_2]^{2+}$[27] and the wheel-like $[Mn_7X_6(mda)_6]^-$ (X = Cl^-, N_3^-) clusters.[28] In the present study, we have investigated the reactions of LH_5 with simple Mn^{II} sources in the absence of carboxylate groups. In some cases, we have in addition included a source of azide ions, which are also excellent bridging ligands and can foster the formation of high nuclearity products.[29]

Various reactions have been systematically explored with differing reagent ratios, reaction solvents, and other conditions. The reaction of $Mn(ClO_4)_2 \cdot 6H_2O$ and NaN_3 with LH_5 and NEt_3 in a 1 : 1 : 1 : 2 molar ratio in DMF gave a brown solution and the subsequent isolation of well-formed red crystals of $[Mn(N_3)(LH_3)] \cdot \frac{1}{2}Et_2O$ (**1**·½Et$_2$O) in high yield (~70%). The formation of **1** is summarized in eqn (1).

$$Mn^{2+} + LH_5 + NEt_3 + N_3^- + \tfrac{1}{4}O_2 \rightarrow [Mn(N_3)(LH_3)] + NHEt_3^+ + \tfrac{1}{2}H_2O \quad (1)$$

The oxidation of Mn^{II} to Mn^{III} is almost certainly by atmospheric O_2 under the slightly basic conditions prevailing. The use of DMF as reaction solvent is crucial for clean product formation; oily products were obtained when the reaction was performed in MeOH, EtOH or MeCN, whereas no significant reaction was observed when the solvent was CH_2Cl_2 or $CHCl_3$. However, complex **1** was obtained using DMSO as reaction solvent but in a much lower yield (~20%). The presence of NEt_3 is also crucial for the clean isolation of **1**, providing a proton acceptor to facilitate the partial deprotonation of LH_5. In an attempt to fully deprotonate LH_5 and thus perhaps obtain higher nuclearity Mn products, several reactions were performed with higher NEt_3:LH_5 ratios, up to 5 : 1. However, complex **1** was still the only isolable product, in comparable (2 : 1 ratio) or lower (3–5 : 1 ratio) yields. No added base at all gave only pale yellow solutions indicative of Mn^{II} products, likely containing the neutral LH_5 ligand.

Since complex **1** was obtained from the presence of NaN_3, we also explored various $Mn(ClO_4)_2/LH_5/NEt_3$ reaction systems in DMF in the absence of azide. These gave dark brown solutions but we have been unable to date to isolate any clean products from these reactions, except when the solvent was MeOH (*vide infra*). With several higher $Mn^{II} : LH_5$ ratios and added base, we again targeted higher-nuclearity products, but in all cases complex **1** was again the only isolable product, in poor yields of 10–20%.

Since we could not easily divert the synthesis of complex **1** to higher nuclearity products, we instead decided to investigate reactions of pre-isolated **1**. Its insolubility in most common solvents limited our choices, and we thus employed MeOH in which **1** is very slightly soluble. Given the only partial deprotonation of LH_3^{2-} in **1**, we targeted its additional deprotonation by reaction of **1** with 1–3 equivalents of base, either NEt_3 or NMe_4OH. Such reactions gave insoluble amorphous powders that perhaps were polymeric, and the filtrates gradually became colorless, indicating the presence of exclusively Mn^{II} species. We thus added additional Mn^{II} to discourage polymer formation, and now the reaction of **1**, NEt_3 and $MnCl_2{\cdot}4H_2O$ in a 2 : 2 : 1 ratio in MeOH (Method A of Experimental section) led to subsequent isolation of well-formed red crystals of $[Mn_5(LH_2)_3(LH_5)(MeOH)_{2.5}]Cl_4$ (**2**) in good yield (~50%). Its formation is summarized in eqn (2).

$$4[Mn(N_3)(LH_3)] + 2Mn^{2+} + NEt_3 + 2\tfrac{1}{2}MeOH \rightarrow 4N_3^- + [Mn_5(LH_2)_3(LH_5)(MeOH)_{2.5}]^{4+} + NHEt_3^+ + Mn^{3+} \quad (2)$$

A similar reaction (Method B) but with extra Mn^{III}, added as the $(NEt_4)_2[MnCl_5]$ salt, and NEt_4OH in place of NEt_3, also gave complex **2** but in a lower yield (~35%).

Once the identity of **2** had been established, we also sought and identified a convenient preparation of **2** in MeOH involving aerial oxidation of simple Mn^{II} starting materials. This was the reaction between $MnCl_2{\cdot}4H_2O$, LH_5 and NEt_3 in a 1 : 1 : 3 ratio in MeOH, which gave **2** in high-yield (~75%); the reaction is summarized in eqn (3).

$$5Mn^{2+} + 4LH_5 + 6NEt_3 + \tfrac{3}{4}O_2 + 2\tfrac{1}{2}MeOH \rightarrow [Mn_5(LH_2)_3(LH_5)(MeOH)_{2.5}]^{4+} + 6NHEt_3^+ + 1.5H_2O \quad (3)$$

Again, an increase in the $NEt_3 : LH_5$ ratio up to 5 : 1 gave comparable (or slightly decreased) yields of complex **2** rather than a higher nuclearity product from complete deprotonation of LH_2^{3-}/LH_5 groups. Further increases in the amount of NEt_3 led to insoluble amorphous precipitates that may be polymers formed from this further deprotonation. Complex **2** was also obtained, but in lower yields (<20%), from reactions with $Mn^{II} : LH_5$ ratios of 2 : 1, 3 : 1, and 1 : 2 in MeOH. Clearly, complex **2** is the preferred product of these reaction components under these conditions.

Structural description of $[Mn(N_3)(LH_3)]$ (1) and $\{[Mn_5(LH_2)_3(LH_5)(MeOH)_3]Cl_4\}\cdot\{[Mn_5(LH_2)_3(LH_5)(MeOH)_2Cl]Cl_3\}$ (2)

A partially labeled representation of complex **1** is shown in Fig. 1. Selected interatomic distances and angles are listed in Table 2. The compound crystallizes in triclinic space group $P\bar{1}$ with the Mn monomer in a general position. The Mn^{III} atom is coordinated by a $\{NO_4\}$-pentadentate chelating LH_3^{2-} group (Scheme 2) and a N-atom from a terminal N_3^- group. Thus, the Mn^{III} atom is six-coordinate with distorted octahedral geometry and exhibits a Jahn–Teller (JT) distortion, as expected for a d^4 ion in near-octahedral geometry. The distortion takes the form of an axial elongation, as is almost always the case for Mn^{III}, with the elongation axis being O(2)–Mn–O(4), as reflected in the two long *trans* bonds (Mn–O2 = 2.208(1) Å and Mn–O4 = 2.235(2) Å). The Mn^{III} oxidation state was confirmed by a bond valence sum (BVS) calculation,[30] which gave a value of 3.07. BVS calculations on the O atoms also confirmed that two of the bound O atoms (O1 and O3) are deprotonated (BVS = 1.78–1.89), whereas the other two bound O atoms (O2 and O4) remain protonated (BVS = 1.34–1.38), as is the unbound O atom O5; *i.e.* the chelate is LH_3^{2-}.

Table 2 Selected interatomic distances (Å) and angles (°) for $\mathbf{1}\cdot\frac{1}{2}Et_2O$

Mn–O1	1.907(1)	Mn–O4	2.235(2)
Mn–O2	2.208(1)	Mn–N1	1.973(2)
Mn–O3	1.876(1)	Mn–N4	2.063(2)
O1–Mn–O3	169.33(6)	O1–Mn–O4	92.04(6)
O1–Mn–N1	93.43(7)	O2–Mn–O4	159.42(6)
O1–Mn–N4	85.70(6)	N1–Mn–N4	177.15(7)

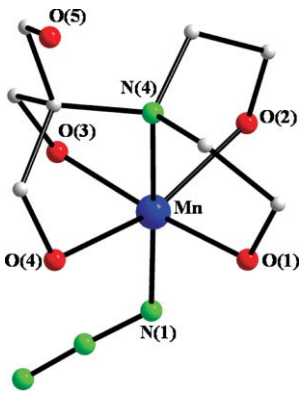

Fig. 1 Labelled PovRay representation of complex **1**, with H atoms omitted for clarity.

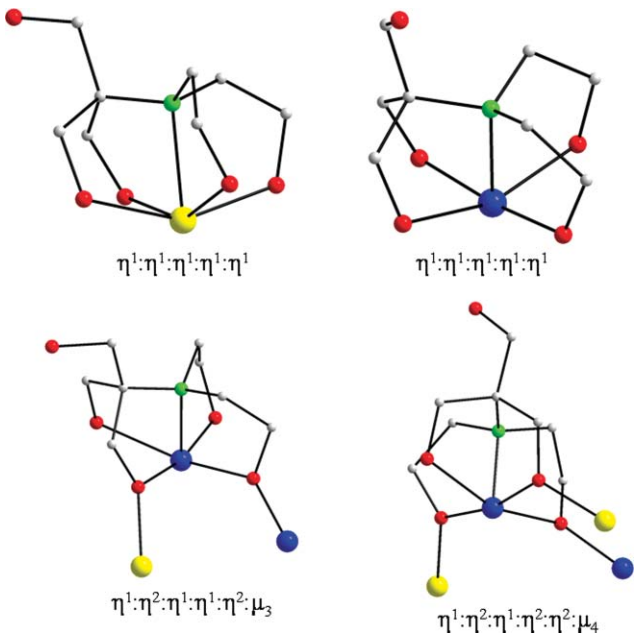

Scheme 2 The coordination modes of LH_5 (top, left), LH_3^{2-} (top, right), and LH_2^{3-} (bottom) in complexes **1** and **2**. Colour scheme: Mn^{II} yellow; Mn^{III} blue; O red; N, green; C grey.

There are three symmetry-inequivalent, intermolecular $OH\cdots O$ hydrogen bonds involving the protonated LH_3^{2-} O atoms being the H-bond donors and the deprotonated LH_3^{2-} O atoms of a neighboring molecule being the acceptors (Fig. 2). Two of these H-bonds, $O(2)\cdots O(3)$ = 2.560(4) Å and $O(4)\cdots O(1)$ = 2.582(4) Å, serve to link neighbouring Mn monomers into one-dimensional, zig-zag chains along the *b* axis. The remaining one,

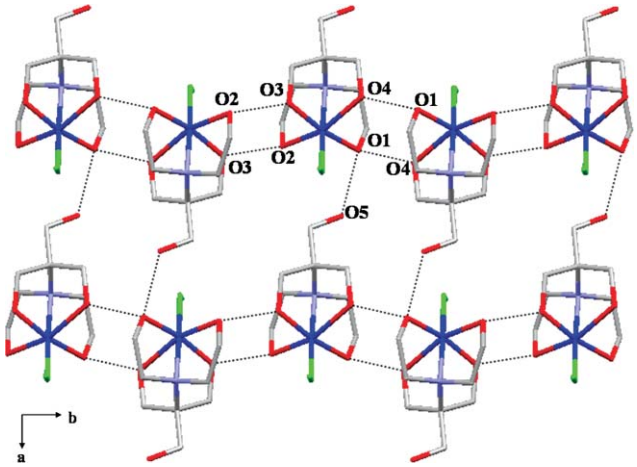

Fig. 2 A partially-labelled section of the 2D hydrogen bonding network of **1** illustrating the inter-chain hydrogen bonding linkages through the LH_3^{2-} groups. Colour scheme: Mn, blue; O, red; N, green; C, grey.

$O(5)\cdots O(1) = 2.758(3)$ Å, serves to link the chains along the crystallographic *a* axis into a 2D sheet structure (Fig. 2). The existence of these many strong hydrogen bonds rationalizes the high thermodynamic stability of **1** leading to its very low solubility in all organic solvents.

Complex **2** crystallizes in the triclinic space group $P\bar{1}$ with two crystallographically independent Mn_5 cations in the asymmetric unit, both in a general position. The two units, $[Mn_5(LH_2)_3(LH_5)(MeOH)_3]Cl_4$ (**2a**) and $[Mn_5(LH_2)_3(LH_5)(MeOH)_2Cl]Cl_3$ (**2b**) are essentially identical, differing only in that a terminal MeOH group of **2a** is replaced by a terminal Cl^- ion in **2b**; as a result, the overall charge of **2a** is 4+, whereas that of **2b** is 3+. Thus, only the structure of **2a** will be further discussed.

The partially labelled structure of the $[Mn_5(LH_2)_3(LH_5)(MeOH)_3]^{4+}$ (**2a**) cation is shown in Fig. 3. Selected interatomic distances and angles are listed in Table 3. The labelled structure

Table 3 Selected interatomic distances (Å) and angles (°) for **2a**

Mn1–O1	1.917(4)	Mn3–O12	2.215(4)
Mn1–O2	2.386(4)	Mn3–O13	2.155(4)
Mn1–O3	1.911(3)	Mn3–O14	2.165(4)
Mn1–O17	1.895(4)	Mn4–O14	1.921(4)
Mn1–O22	2.118(4)	Mn4–O15	2.474(4)
Mn1–N1	2.057(4)	Mn4–O16	1.885(4)
Mn2–O3	2.080(3)	Mn4–O17	2.148(3)
Mn2–O5	2.202(5)	Mn4–O21	1.879(4)
Mn2–O6	2.214(5)	Mn4–N3	2.053(4)
Mn2–O7	2.151(5)	Mn5–O13	1.926(4)
Mn2–O8	2.219(5)	Mn5–O19	2.355(4)
Mn2–N2	2.314(5)	Mn5–O20	1.866(4)
Mn3–O1	2.184(3)	Mn5–O21	2.161(4)
Mn3–O10	2.242(4)	Mn5–O22	1.897(3)
Mn3–O11	2.239(4)	Mn5–N4	2.059(4)
Mn1···Mn2	3.533(2)	Mn2···Mn4	4.813(4)
Mn1···Mn3	3.701(3)	Mn2···Mn5	4.863(3)
Mn1···Mn4	3.710(2)	Mn3···Mn4	3.667(2)
Mn1···Mn5	3.673(2)	Mn3···Mn5	3.662(2)
Mn2···Mn3	6.728(4)	Mn4···Mn5	3.753(2)
Mn1–O3–Mn2	124.5(2)	Mn3–O14–Mn4	127.5(2)
Mn1–O1–Mn3	128.8(2)	Mn3–O13–Mn5	127.5(2)
Mn1–O17–Mn4	133.0(2)	Mn4–O21–Mn5	136.5(2)
Mn1–O22–Mn5	132.3(2)		

and interatomic distances and angles for complex **2b** are shown in Fig. S1 and Table S1, respectively, in the ESI.† The core of **2a** consists of five Mn atoms arranged in a distorted trigonal bipyramidal topology (Fig. 4, top). The apical positions are occupied by two Mn^{II} ions, whereas three Mn^{III} ions reside in the equatorial trigonal plane. The Mn_{eq}–Mn_{eq}–Mn_{eq}, Mn_{eq}–Mn_{eq}–Mn_{ap}, and Mn_{eq}–Mn_{ap}–Mn_{eq} angles range from 59.0(2)–61.1(2)°, 59.1(2)–84.9(2)°, and 45.6(2)–61.6(2)°, respectively. Each Mn^{III} ion is linked by three monoatomic RO^- bridges (O1, O13, O14) of three LH_2^{3-} groups to one of the apical Mn^{II} (Mn3) atoms. The only

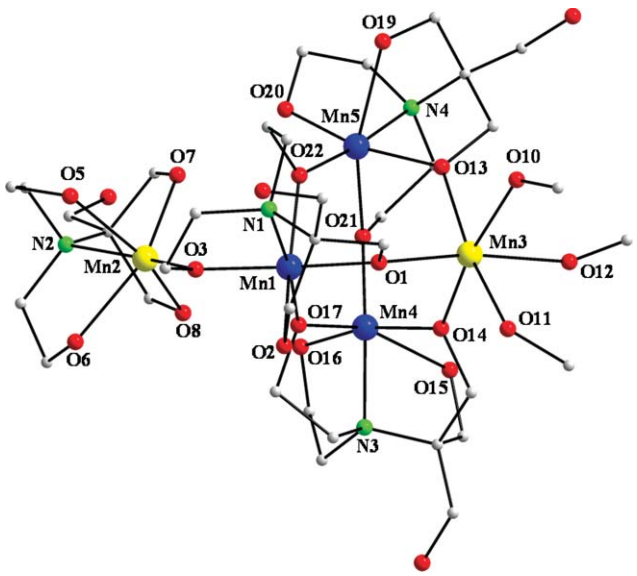

Fig. 3 Labelled PovRay representation of the cation **2a**, with H atoms omitted for clarity. Colour scheme: Mn^{II} yellow; Mn^{III} blue; O red; N green; C grey.

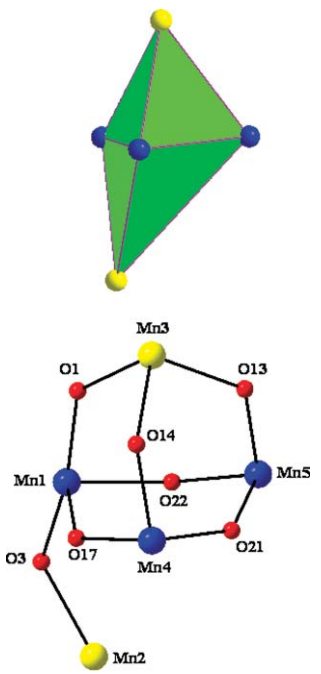

Fig. 4 (top) The Mn_5 topology of **2a**, emphasizing the trigonal bipyramidal description. (bottom) PovRay representation of the complete $[Mn_5(\mu\text{-}OR)_7]^{6+}$ core. Colour scheme: Mn^{II} yellow; Mn^{III} blue; O red.

linkage between an equatorial Mn^{III} ion (Mn1) and the remaining apical Mn^{II} atom (Mn2) is provided by another monoatomic RO^- bridge (O3) from an LH_2^{3-} group. The three Mn^{III} centers are bridged by three RO^- groups (O17, O21, O22), one each from the three LH_2^{3-} chelates. Two of the latter are pentadentate-chelating to a Mn^{III} atom, with two of their three deprotonated RO^- arms bridging to an adjacent Mn^{II} and Mn^{III} atom; these groups are thus $\eta^1:\eta^2:\eta^1:\eta^1:\eta^2:\mu_3$ (Scheme 2). The remaining LH_2^{3-} group is also pentadentate-chelating to a Mn^{III} atom, but in this case all three deprotonated RO^- arms bridge to adjacent Mn^{II} and Mn^{III} atoms; this group is thus $\eta^1:\eta^2:\eta^1:\eta^2:\eta^2:\mu_4$ (Scheme 2). In addition, there is one neutral LH_5 group acting as a pentadentate chelate (Scheme 2) to Mn^{II} atom Mn2, and three terminal MeOH molecules bound to the other Mn^{II} atom Mn3. The complex thus contains a $[Mn_5(\mu\text{-}OR)_7]^{6+}$ core (Fig. 4, bottom).

All Mn atoms are six-coordinate with distorted octahedral geometry. Charge considerations and an inspection of the metric parameters indicate a $2Mn^{II}$, $3Mn^{III}$ description, which was confirmed quantitatively by BVS calculations (Table 4),[30] which identified Mn2 and Mn3 as the Mn^{II} ions, and the others as Mn^{III}. The latter also show a Jahn–Teller axial elongation, with alkoxide oxygen atoms O2/O22, O15/O17, and O19/O21 of the LH_2^{3-} groups occupying the axial positions of the Mn1, Mn4 and Mn5 distorted octahedra, respectively. The protonation levels of the peripheral and bridging RO^- groups of LH_2^{3-} were also confirmed by BVS calculations (Table 4).

In addition to the trigonal bipyramidal description of **2a**, an alternative way of describing it can be presented that emphasizes its structural relationship to $[Mn(N_3)(LH_3)]$ (**1**). The $\{[Mn_4(LH_2)_3(LH_5)][Mn(MeOH)_3]\}^{4+}$ (**2a**) cation can be considered as four $MnNO_5$ octahedra of mononuclear $\{Mn(LH_x)\}$ units linked together, and to the fifth $\{Mn(MeOH)_3\}$ unit, through the deprotonated oxygen atoms of LH_2^{3-} groups.

Complex **2a** contains two strong intramolecular hydrogen bonds between two of the protonated OH groups of the LH_5 chelate and the terminal, deprotonated RO^- groups of two neighboring LH_2^{3-} chelates ($O(7)\cdots O(20) = 2.567(4)$ Å, $O(8)\cdots O(16) = 2.574(4)$ Å). There are also many hydrogen bonds between the many protonated OH groups of LH_5/LH_2^{3-} ligands and the Cl^- counterions, with $O\cdots Cl$ distances in the 3.0–3.1 Å range, or slightly greater. These serve to link neighboring Mn_5 cations and Cl^- anions in the crystal into a 3D H-bonded network.

Table 4 Bond valence sum (BVS)[a,b] calculations for Mn and selected oxygen atoms in **2a**

Atom	Mn^{II}	Mn^{III}	Mn^{IV}
Mn1	3.183	**2.942**	3.039
Mn2	**1.961**	1.809	1.874
Mn3	**1.860**	1.701	1.786
Mn4	3.192	**2.951**	3.048
Mn5	3.221	**2.977**	3.076
	BVS	Assignment	
O1	1.74	RO^-	
O3	1.86	RO^-	
O13	1.78	RO^-	
O14	1.75	RO^-	
O16[c]	1.50	RO^-	
O17	1.77	RO^-	
O20[c]	1.56	RO^-	
O21	1.81	RO^-	
O22	1.80	RO^-	

[a] The bold value is the one closest to the charge for which it was calculated. The oxidation state of a particular atom is the nearest whole number to the bold value. [b] A BVS in the ~1.8–2.0, ~1.0–1.2, and ~0.2–0.4 ranges for an O atom is indicative of non-, single- and double-protonation, respectively, but can be altered somewhat by H- bonding. [c] Non-bridging, deprotonated O atoms.

Complex **2** joins a small family of cage-like Mn clusters of nuclearity five. Many of these have been reported only within the last several years, and they are listed in Table 5 for a convenient comparison of their structural type and pertinent magnetic data such as ground state spin (*S*) values (*vide infra*). Examination of Table 5 shows that complex **2** is one of six Mn_5 trigonal pyramids currently known; three of these are wholly Mn^{II} species, and there are only two at the $Mn^{II}_2Mn^{III}_3$ oxidation level, complex **2** and the anion $[Mn^{II}_2Mn^{III}_3O(salox)_3Cl_2(N_3)_6]^{3-}$.

Magnetochemistry

Magnetic susceptibility studies on complex 1. Variable-temperature magnetic susceptibility measurements were

Table 5 Structural types and ground state *S* values for pentanuclear Mn clusters[a]

Complex[b]	Core	Type	*S*	Ref.
$[Mn^{II}_5(Htrz)_2(SO_4)_4(OH)_2]$	$[Mn_5(\mu_3\text{-}OH)_2]^{8+}$	*c*	n.r.	31
$[Mn^{II}_5(p3oapH)_6]^{4+}$	$[Mn_5(\mu\text{-}OR)_6]^{4+}$	*d*	5/2	32
$[Mn^{II}_5(poapH)_6]^{4+}$	$[Mn_5(\mu\text{-}OR)_6]^{4+}$	*d*	5/2	32
$[Mn^{II}_5(L)_2(O_2CMe)_2(ClO_4)_2]^{2+}$	$[Mn_5(\mu\text{-}OR)_6(\mu\text{-}OClO_3)_2]^{2+}$	*e*	n.r.	33
$[Mn^{II}_5(phaapH)_6]^{4+}$	$[Mn_5(\mu\text{-}OR)_6]^{4+}$	*d*	5/2	34
$[Mn^{II}Mn^{III}_4(shi)_4(O_2CMe)_2(DMF)_6]$	$[Mn_5(\mu_3\text{-}ON)_4]^{10+}$	*f*	n.r.	35
$[Mn^{II}Mn^{III}_4(shi)_4(O_2CPh)_2(MeOH)_6]$	$[Mn_5(\mu_3\text{-}ON)_4]^{10+}$	*f*	n.r.	36
$[Mn^{II}_2Mn^{III}_3O(salox)_3Cl_2(N_3)_6]^{3-}$	$[Mn_5(\mu_3\text{-}O)(\mu\text{-}ON)_3(\mu\text{-}N_3)_6]^{2+}$	*d*	11	37
$[Mn^{II}_2Mn^{III}_3(LH_2)_3(LH_5)(MeOH)_3]^{4+}$ (**2**)	$[Mn_5(\mu\text{-}OR)_7]^{6+}$	*d*	2	t.w.
$[Mn^{II}_3Mn^{III}_2(fsatren)_2(H_2O)_4]$	$[Mn_5(\mu\text{-}OR)_8]^{4+}$	*g*	7/2	38
$[Mn^{II}_3Mn^{III}_2(tmphen)_6(CN)_{12}]$	$[Mn_5(\mu\text{-}NC)_6]^{6+}$	*d*	11/2	39
$[Mn^{II}_4Mn^{III}(cat)_4(O_2CCMe_3)_2(py)_8]^+$	$[Mn_5(\mu_3\text{-}OR)_4(\mu\text{-}OR)_4]^{3+}$	*e*	n.r.	40

[a] Abbreviations: n.r. = not reported; t.w. = this work; Htrz = triazole; poapH, p3oapH, phaapH = ditopic, diazine ligands; LH_2 = a [2 + 2] macrocycle; $shiH_3$ = salicylhydroxamic acid; DMF = dimethylformamide; $saloxH_2$ = salicylaldoxime; $fsatrenH_6$ = 3-formylsalicylic acid; tmphen = 3,4,7,8-tetramethyl-1,10-phenanthroline; $catH_2$ = catechol; py = pyridine. [b] Counterions and solvate molecules are omitted. [c] Edge-sharing MnO_6 octahedra. [d] Trigonal bipyramid. [e] Four Mn around a central Mn. [f] [12-metallacrown-4]∩Mn ring. [g] Linear array.

performed on a powdered polycrystalline sample of **1**, restrained in icosane to prevent torquing, in a 1 kG (0.1 T) field and in the 5.0–300 K range. The obtained data are shown as a $\chi_M T$ *vs.* T plot in Fig. 5. $\chi_M T$ remains almost constant at a value of ~3.0–3.1 cm^3 K mol^{-1} as the temperature decreases, until ~40.0 K where the value starts to decrease sharply to a minimum value of 1.86 cm^3 K mol^{-1} at 5.0 K. The 40–300 K data are consistent with an $S = 2$ spin state, as expected for a high-spin d^4 Mn^{III} complex in near-octahedral geometry; the spin-only ($g = 2$) value for $S = 2$ is 3.00 cm^3 K mol^{-1}. The low-temperature (<40.0 K) decrease is attributed to both a combination of a zero-field splitting, D, expected for a Mn^{III} atom in a Jahn–Teller distorted octahedral arrangement, and intermolecular antiferromagnetic interactions between neighboring molecules of **1** (*vide infra*). The latter must be considered to be weak but not negligible given the H-bonding that is present between neighbouring molecules of **1** in the crystal.

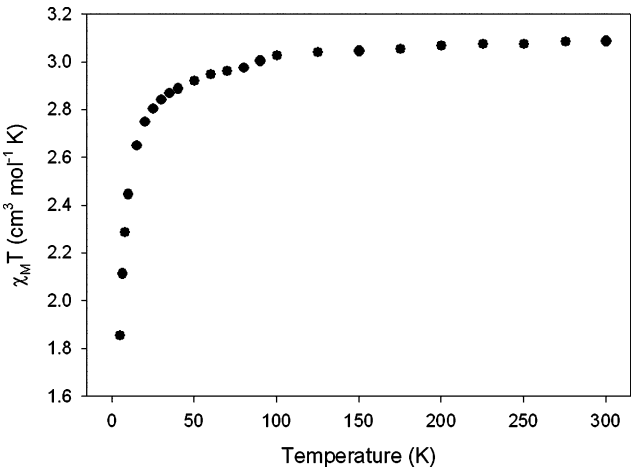

Fig. 5 Plot of $\chi_M T$ *vs.* T for complex **1**.

The structural data for **1**, namely its Jahn–Teller elongation, strongly support a $^5B_{1g}$ ground state (using octahedral symmetry labels),[41] and hence a negative ZFS parameter D. We probed this further to determine the magnitude and sign of D by fitting magnetization (M) data collected over a range of magnetic fields. Thus, M *vs.* dc field measurements were made on restrained samples in the magnetic field (H) and temperature ranges of 1–70 kG and 1.8–10.0 K, respectively. The strong fields employed are expected to overcome the effect of weak intermolecular interactions. The resulting data for **1** are shown in Fig. 6 as a reduced magnetization ($M/N\mu_B$) *vs.* H/T plot, where N is Avogadro's number and μ_B is the Bohr magneton. The data were fit using the program MAGNET[23a] to a model that assumes only that the ground state is populated at these temperatures and magnetic fields, includes isotropic Zeeman interactions and axial zero-field splitting ($D\hat{S}_z^2$), and incorporates a full powder average. The corresponding spin Hamiltonian is given by eqn (4)

$$\mathscr{H} = D\hat{S}_z^2 + g\mu_B\mu_0\hat{S}H, \quad (4)$$

where $\hat{S}_z$ is the easy-axis spin operator, and μ_0 is the vacuum permeability. The last term in eqn (4) is the Zeeman energy associated with an applied magnetic field. The best fit is shown as the solid lines in Fig. 6 and was obtained with $S = 2$, $g = 1.85(4)$, and $D = -2.75(7)$ cm^{-1}; the fit was noticeably worse when

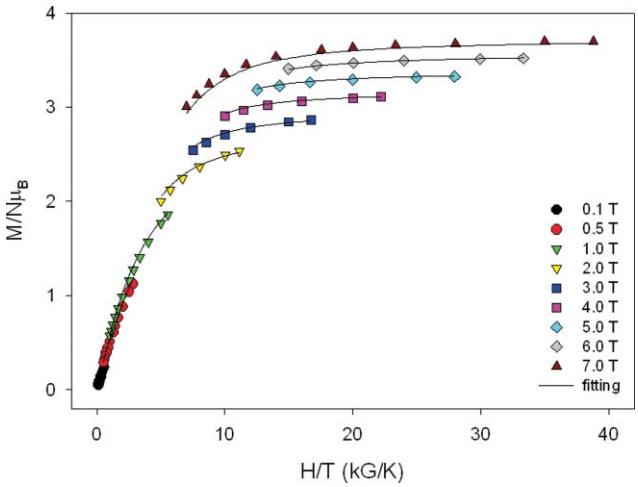

Fig. 6 Magnetization (M) *vs.* field (H) and temperature (T) data, plotted as reduced magnetization ($M/N\mu_B$) *vs.* H/T, for complex **1** at applied fields of 0.1–7.0 T and in the 1.8–10 K temperature range. The solid lines are the fit of the data; see the text for the fit parameters.

positive values of D were employed. The root-mean-square D *vs.* g error surface for the fit was generated using the program GRID,[23a] which calculates the relative difference between the experimental $M/N\mu_B$ data and those calculated for various combinations of D and g. The obtained error surface (Fig. S2†) shows the best fit to be the global minimum, and to be a fairly hard minimum, indicating a relatively small level of uncertainty in the fit parameters.

The obtained value of $|D|$ is, however, somewhat smaller than those reported for other mononuclear, octahedral Mn^{III} complexes,[41,42] which are typically 3.2 cm^{-1} or greater for N and/or O ligation. In fact, the value for **1** is in the range normally found for five-coordinate Mn^{III} complexes with square pyramidal geometries.[43] We therefore suspected that the smaller than expected D value was an artifact due to the large distortion of complex **1** from octahedral geometry, leading to a significant rhombic zero-field splitting parameter E. Thus, we included both D and E in the magnetization fit for **1**; shown in Fig 7 is the error surface for this D *vs.* E fit with a fixed $g = 2.0$. The best fit was with $D = -3.25$ cm^{-1} and $|E| = 0.32$ cm^{-1}. These parameters are quite similar to those previously determined by electron paramagnetic spectroscopy for another Mn^{III} azide complex [Mn(terpy)$(N_3)_3$] ($D = -3.29$ cm^{-1}, $|E| = 0.51$ cm^{-1}, $g = 2.00$).[44]

Magnetic susceptibility studies on complex 2. Variable-temperature magnetic susceptibility measurements were performed on a microcrystalline powder sample of **2**, restrained in icosane to prevent torquing, in a 1 kG (0.1 T) field and in the 5.0–300 K range. The obtained data are shown as a $\chi_M T$ *vs.* T plot in Fig. 8. $\chi_M T$ rapidly decreases from 17.44 cm^3 K mol^{-1} at 300 K to 4.45 cm^3 K mol^{-1} at 5.0 K. The 300 K value is slightly less than the spin-only ($g = 2$) value of 17.75 cm^3 K mol^{-1} for two Mn^{II} and three Mn^{III} non-interacting ions, indicating the presence of dominant antiferromagnetic exchange interactions. The 5.0 K value is more consistent with an $S = 3$ rather than an $S = 2$ ground state, since the g factor should be slightly less than 2.0 for a Mn^{II}/Mn^{III} complex; the spin-only values for $S = 3$ and $S = 2$ are 6.00 and 3.00 cm^3 K mol^{-1}, respectively. Given the low-symmetry of the Mn_5 cation, and the resulting number of inequivalent exchange constants,

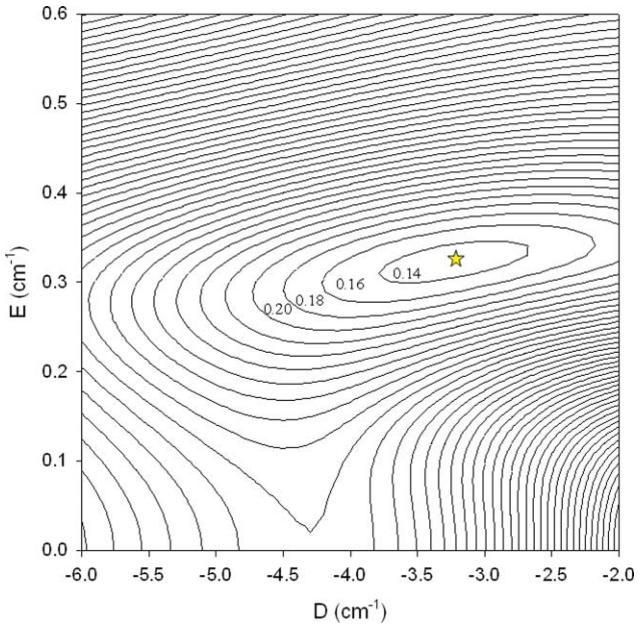

Fig. 7 Two-dimensional contour plot of the root-mean-square error surface for the D *vs.* E fit for complex **1** with a fixed $g = 2.0$. The star indicates the best fit (error minimum); see the text for the fit parameters.

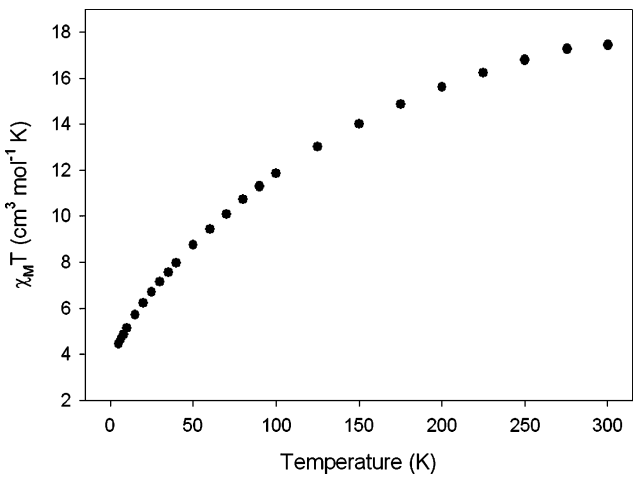

Fig. 8 Plot of $\chi_M T$ *vs.* T for complex **2**.

it is unreliable to apply the Kambe method[45] to determine the individual pairwise Mn_2 exchange interaction parameters, and we concentrated instead only on characterizing the ground state spin, S, and the zero-field splitting parameter, D. Magnetization (M) *vs.* dc field measurements were made on restrained samples in the magnetic field (H) and temperature ranges of 1–60 kG and 1.8–10.0 K, respectively. The resulting data for **2** are shown in Fig. 9 as a reduced magnetization ($M/N\mu_B$) *vs.* H/T plot. The data were fit using the program MAGNET,[23a] as described above for the fit for complex **1**. The best fit is shown as the solid lines in Fig. 9 and was obtained with $S = 3$, $g = 1.88(2)$, and $D = -0.68(1)$ cm^{-1}. Alternative fits with $S = 2$ or 4 were rejected because they gave unreasonable values of g and D.

As we have described before on multiple occasions,[6,15,46] ac susceptibility studies are a powerful complement to dc studies for determining the ground state of a system, because they

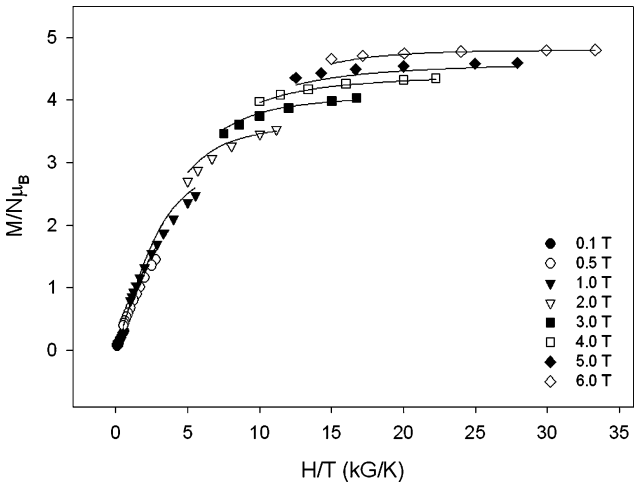

Fig. 9 Magnetization (M) *vs.* field (H) and temperature (T) data, plotted as reduced magnetization ($M/N\mu_B$) *vs.* H/T, for complex **2** at applied fields of 0.1–6.0 T and in the 1.8–10 K temperature range. The solid lines are the fit of the data; see the text for the fit parameters.

preclude any complications arising from the presence of a dc field. We thus chose to carry out ac studies on complex **2** as an independent determination of its ground state S. These were performed in the 1.8–15 K range using a 3.5 G ac field oscillating at frequencies in the 50–1000 Hz range. If the magnetization vector can relax fast enough to keep up with the oscillating field, then there is no imaginary (out-of-phase) susceptibility signal (χ''_M), and the real (in-phase) susceptibility (χ'_M) is equal to the dc susceptibility. However, if the barrier to magnetization relaxation is significant compared to thermal energy (kT), then the in-phase signal decreases and a non-zero, frequency-dependent χ''_M signal appears, which is suggestive of the superparamagnetic-like properties of a SMM. For complex **2**, the in-phase $\chi'_M T$ *vs.* T data are shown in Fig. 10 and show a rapid decrease below 10 K consistent with decreasing population of low-lying excited states with S greater than that of the ground state. Extrapolation of the plot to 0 K from above 6 K (to avoid the decrease at lower T due to anisotropy, Zeeman effects, weak intermolecular

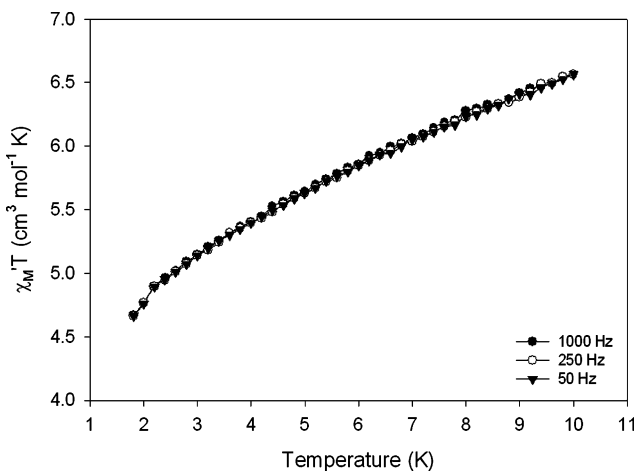

Fig. 10 Plot of the in-phase ac susceptibility signals, $\chi'_M T$ *vs.* T for complex **2** at the indicated frequencies.

interactions, *etc.*) gives a value of ~5.0 cm^3 K mol^{-1}. This indicates an $S = 3$ ground state with a $g \sim 1.83$, in general agreement with the dc magnetization fit. Note that $S = 2$ and 4 ground states would be expected to give $\chi'_M T$ values of slightly less than 3 and 10 cm^3 K mol^{-1}, respectively, clearly very different from the experimental values. The slightly low value of g, which would normally be expected in the 1.90–2.00 range, is most probably due to experimental error, particularly the difficulty in achieving an accurate extrapolation in the presence of ZFS and intermolecular interactions. Nevertheless, this does not impact on our overall conclusion that complex **2** does indeed have an $S = 3$ ground state. Finally, complex **2** did not exhibit an out-of-phase ac magnetic susceptibility signal down to 1.8 K, indicating that it does not exhibit a barrier large enough (*vs.* kT) to show the superparamagnet-like slow relaxation of its magnetization vector, *i.e.* it is not a SMM. Studies at much lower temperatures would be required to search for what would at best be a tiny relaxation barrier.

The $S = 3$ ground state of $2Mn^{II}$, $3Mn^{III}$ complex **2** has not been previously encountered in Mn_5 clusters, and it is distinctly different from the $S = 11$ ground state possessed by the entirely ferromagnetic $[Mn^{II}_2Mn^{III}_3O(salox)_3Cl_2(N_3)_6]^{3-}$ complex mentioned above that also has a trigonal bipyramidal Mn_5 topology.[37] An $S = 3$ ground state for a $2Mn^{II}$, $3Mn^{III}$ complex such as **2** that has spin values in the $S = 0$–11 range is consistent with the presence of spin frustration effects arising from antiferromagnetic coupling within the several triangular units in the structure. There are thus various possible coupling schemes and resulting intermediate spin alignments at some metals that could yield an $S = 3$ ground state, making it difficult to rationalize the observed value in a unique manner without recourse to theoretical calculations. Note however that some coupling schemes can clearly be ruled out, such as the ferromagnetic $J(Mn^{III}Mn^{III})$ and antiferromagnetic $J(Mn^{II}Mn^{III})$ possibility, which would give an $S = 1$ ground state.

Conclusions

We have reported the employment of 'bis-tris' (LH_5) as a new, potentially $\{NO_5\}$-based hexadentate ligand in manganese cluster chemistry, one that can be thought of as an amalgamation of $thmeH_3$ and $mdaH_2$. In the present work, it has bound as a $\{NO_4\}$-chelating and bridging ligand, the fifth OH group remaining protonated and unbound, but the hexadentate binding mode will likely be encountered as the coordination chemistry of LH_5 is further developed. The versatility of this reagent is suggested by the products of this initial study, both a mononuclear Mn^{III} species and a Mn_5 cluster, emphasizing again the ability of poly-ol groups to foster formation of high nuclearity products. It will be interesting to determine, as this work is extended, to what extent the LH_5 ligand will continue to provide a route to new metal clusters and to what extent, if any, these are related to clusters provided by dipodal (mda^{2-}) and tripodal ($thme^{3-}$) ligands alone.

Acknowledgements

This work was supported by the National Science Foundation (CHE-0414555).

References

1 (*a*) X.-J. Wang, T. Langetepe, C. Persau, B.-S. Kang, G. M. Sheldrick and D. Fenske, *Angew. Chem., Int. Ed.*, 2002, **41**, 3818; (*b*) M. Cavallini, J. Gomez-Segura, D. Ruiz-Molina, M. Massi, C. Albonetti, C. Rovira, J. Veciana and F. Biscarini, *Angew. Chem., Int. Ed.*, 2005, **44**, 888.
2 K. N. Ferreira, T. M. Iverson, K. Maghlaoui, J. Barber and S. Iwata, *Science*, 2004, **303**, 1831; T. G. Carrell, A. M. Tyryshkin and G. C. Dismukes, *JBIC, J. Biol. Inorg. Chem.*, 2002, **7**, 2; R. M. Cinco, A. Rompel, H. Visser, G. Aromi, G. Christou, K. Sauer, M. P. Klein and V. K. Yachandra, *Inorg. Chem.*, 1999, **38**, 5988; V. K. Yachandra, K. Sauer and M. P. Klein, *Chem. Rev.*, 1996, **96**, 2927; A. Mishra, W. Wernsdorfer, K. A. Abboud and G. Christou, *Chem. Commun.*, 2005, 54.
3 For reviews, see: G. Christou, D. Gatteschi, D. N. Hendrickson and R. Sessoli, *MRS Bull.*, 2000, **25**, 66; G. Aromi and E. K. Brechin, *Struct. Bonding*, 2006, **122**, 1.
4 R. Bircher, G. Chaboussant, C. Dobe, H. U. Güdel, S. T. Ochsenbein, A. Sieber and O. Waldmann, *Adv. Funct. Mater.*, 2006, **16**, 209; D. Gatteschi and R. Sessoli, *Angew. Chem., Int. Ed.*, 2003, **42**, 268; S. M. J. Aubin, N. R. Gilley, L. Pardi, J. Krzystek, M. W. Wemple, L.-C. Brunel, M. B. Maple, G. Christou and D. N. Hendrickson, *J. Am. Chem. Soc.*, 1998, **120**, 4991; H. Oshio and M. Nakano, *Chem.–Eur. J.*, 2005, **11**, 5178.
5 G. Christou, *Polyhedron*, 2005, **24**, 2065, and references therein.
6 For example, see: M. Soler, W. Wernsdorfer, K. Folting, M. Pink and G. Christou, *J. Am. Chem. Soc.*, 2004, **126**, 2156; M. Murugesu, M. Habrych, W. Wernsdorfer, K. A. Abboud and G. Christou, *J. Am. Chem. Soc.*, 2004, **126**, 4766; M. Soler, E. Rumberger, K. Folting, D. N. Hendrickson and G. Christou, *Polyhedron*, 2001, **20**, 1365; M. Murugesu, W. Wernsdorfer, K. A. Abboud and G. Christou, *Polyhedron*, 2005, **24**, 2894.
7 A. J. Tasiopoulos, A. Vinslava, W. Wernsdorfer, K. A. Abboud and G. Christou, *Angew. Chem., Int. Ed.*, 2004, **43**, 2117.
8 P. Artus, C. Boskovic, Y. Yoo, W. E. Streib, L.-C. Brunel, D. N. Hendrickson and G. Christou, *Inorg. Chem.*, 2001, **40**, 4199; D. Ruiz, Z. Sun, B. Albela, K. Folting, J. Ribas, G. Christou and D. N. Hendrickson, *Angew. Chem., Int. Ed. Engl.*, 1998, **37**, 300; S. M. J. Aubin, Z. Sun, I. A. Guzei, A. L. Rheingold, G. Christou and D. N. Hendrickson, *Chem. Commun.*, 1997, 2239; C. Boskovic, M. Pink, J. C. Huffman, D. N. Hendrickson and G. Christou, *J. Am. Chem. Soc.*, 2001, **123**, 9914; M. Soler, P. Artus, K. Folting, J. C. Huffman, D. N. Hendrickson and G. Christou, *Inorg. Chem.*, 2001, **40**, 4902.
9 S. Wang, J. C. Huffman, K. Folting, W. E. Streib, E. Lobkovsky and G. Christou, *Angew. Chem., Int. Ed. Engl.*, 1991, **30**, 1672; L. Tsai, S. Wang, K. Folting, W. E. Streib, D. N. Hendrickson and G. Christou, *J. Am. Chem. Soc.*, 1995, **117**, 2503; M. Murugesu, K. A. Abboud and G. Christou, *Polyhedron*, 2004, **23**, 2779.
10 S. Bhaduri, A. Tasiopoulos, M. Pink, K. A. Abboud and G. Christou, *Chem. Commun.*, 2002, 2352; C. Canada-Vilalta, M. Pink and G. Christou, *Dalton Trans.*, 2003, 1121.
11 H.-J. Eppley, H.-L. Tsai, N. de Vries, K. Folting, G. Christou and D. N. Hendrickson, *J. Am. Chem. Soc.*, 1995, **117**, 301; N. E. Chakov, M. Soler, W. Wernsdorfer, K. A. Abboud and G. Christou, *Inorg. Chem.*, 2005, **44**, 5304; S. M. J. Aubin, Z. Sun, L. Pardi, J. Krzystek, K. Folting, L.-C. Brunel, A. L. Rheingold, G. Christou and D. N. Hendrickson, *Inorg. Chem.*, 1999, **38**, 5329; M. Soler, W. Wernsdorfer, K. A. Abboud, J. C. Huffman, E. R. Davidson, D. N. Hendrickson and G. Christou, *J. Am. Chem. Soc.*, 2003, **125**, 3576; M. Soler, S. K. Chandra, D. Ruiz, E. R. Davidson, D. N. Hendrickson and G. Christou, *Chem. Commun.*, 2000, 2417; A. J. Tasiopoulos, W. Wernsdorfer, K. A. Abboud and G. Christou, *Polyhedron*, 2005, **24**, 2505.
12 N. Aliaga, K. Folting, D. N. Hendrickson and G. Christou, *Polyhedron*, 2001, **20**, 1273.
13 S. P. Perlepes, J. C. Huffman and G. Christou, *J. Chem. Soc., Chem. Commun.*, 1991, **23**, 1657.
14 C. Canada-Vilalta, J. C. Huffman and G. Christou, *Polyhedron*, 2001, **20**, 1785; A. G. Harter, C. Lampropoulos, M. Murugesu, P. Kuhns, A. Reyes, G. Christou and N. S. Dalal, *Polyhedron*, 2007, **26**, 2320; S.-C. Lee, Th. C. Stamatatos, S. Hill, S. P. Perlepes and G. Christou, *Polyhedron*, 2007, **26**, 2225; Th. C. Stamatatos, D. Foguet-Albiol, C. C. Stoumpos, C. P. Raptopoulou, A. Terzis, W. Wernsdorfer, S. P. Perlepes and G. Christou, *Polyhedron*, 2007, **26**, 2165.
15 For representative recent work from our group, see: Th. C. Stamatatos, K. A. Abboud, W. Wernsdorfer and G. Christou, *Angew. Chem., Int.*

Ed., 2006, **45**, 4134; Th. C. Stamatatos, K. A. Abboud, W. Wernsdorfer and G. Christou, *Angew. Chem., Int. Ed.*, 2007, **46**, 884; P. King, Th. C. Stamatatos, K. A. Abboud and G. Christou, *Angew. Chem., Int. Ed.*, 2006, **45**, 7379; R. Bagai, K. A. Abboud and G. Christou, *Chem. Commun.*, 2007, 3359; D. Foguet-Albiol, K. A. Abboud and G. Christou, *Chem. Commun.*, 2005, 4282; E. K. Brechin, E. C. Sanudo, W. Wernsdorfer, C. Boskovic, J. Yoo, D. N. Hendrickson, A. Yamaguchi, H. Ishimoto, T. R. Concolino, A. L. Rheingold and G. Christou, *Inorg. Chem.*, 2005, **44**, 502; Th. C. Stamatatos, K. A. Abboud, W. Wernsdorfer and G. Christou, *Polyhedron*, 2007, **26**, 2095; Th. C. Stamatatos, K. A. Abboud, W. Wernsdorfer and G. Christou, *Polyhedron*, 2007, **26**, 2042; E. C. Sanudo, E. K. Brechin, C. Boskovic, W. Wernsdorfer, J. Yoo, A. Yamaguchi, T. R. Concolino, K. A. Abboud, A. L. Rheingold, H. Ishimoto, D. N. Hendrickson and G. Christou, *Polyhedron*, 2003, **22**, 2267.

16 For some representative references, see: R. E. P. Winpenny, *J. Chem. Soc., Dalton Trans.*, 2002, 1; E. K. Brechin, *Chem. Commun.*, 2005, 5141; C. J. Milios, Th. C. Stamatatos and S. P. Perlepes, *Polyhedron*, 2006, **25**, 134 (Polyhedron Report); G. S. Papaefstathiou and S. P. Perlepes, *Comments Inorg. Chem.*, 2002, 249; E. E. Moushi, Th. C. Stamatatos, W. Wernsdorfer, V. Nastopoulos, G. Christou and A. J. Tasiopoulos, *Angew. Chem., Int. Ed.*, 2006, **45**, 7722; M. Manoli, C. J. Milios, A. Mishra, G. Christou and E. K. Brechin, *Polyhedron*, 2007, **26**, 1923; M. Murugesu, W. Wernsdorfer, G. Christou and E. K. Brechin, *Polyhedron*, 2007, **26**, 1845.

17 M. Murugesu, J. Raftery, W. Wernsdorfer, G. Christou and E. K. Brechin, *Inorg. Chem.*, 2004, **43**, 4203; E. Moushi, C. Lampropoulos, W. Wernsdorfer, V. Nastopoulos, G. Christou and A. J. Tasiopoulos, *Inorg. Chem.*, 2007, **46**, 3795; M. Manoli, A. Prescimone, R. Bagai, A. Mishra, M. Murugesu, S. Parsons, W. Wernsdorfer, G. Christou and E. K. Brechin, *Inorg. Chem.*, 2007, **46**, 6968; T. W. R. Scott, S. Parsons, M. Murugesu, W. Wernsdorfer, G. Christou and E. K. Brechin, *Angew. Chem., Int. Ed.*, 2005, **44**, 6540; E. K. Brechin, M. Soler, J. Davidson, D. N. Hendrickson, S. Parsons and G. Christou, *Chem. Commun.*, 2002, 2252; A. M. Ako, I. J. Hewitt, V. Mereacre, R. Clérac, W. Wernsdorfer, C. E. Anson and A. K. Powell, *Angew. Chem., Int. Ed.*, 2006, **45**, 4926; M. Murugesu, W. Wernsdorfer, K. A. Abboud and G. Christou, *Angew. Chem., Int. Ed.*, 2005, **44**, 892; S. Koizumi, M. Nihei, T. Shiga, M. Nakano, H. Nojiri, R. Bircher, O. Waldmann, S. Ochsenbein, H. U. Güedel, F. Fernandez-Alonso and H. Oshio, *Chem.–Eur. J.*, 2007, **13**, 8445.

18 Y. Inomata, Y. Gochou, M. Nogami, F. S. Howell and T. Takeuchi, *J. Mol. Struct.*, 2004, **702**, 61.

19 A. Ferguson, A. Parkin and M. Murrie, *Dalton Trans.*, 2006, 3627.

20 S. P. Perlepes, A. G. Blackman, J. C. Huffman and G. Christou, *Inorg. Chem.*, 1991, **30**, 1665.

21 *SHELXTL6*, Bruker-AXS, Madison, WI, USA, 2000.

22 P. Van der Sluis and A. L. Spek, *Acta Crystallogr. Sect. A: Found. Crystallogr.*, 1990, **46**, 194.

23 (*a*) E. R. Davidson, *MAGNET*, Indiana University, Bloomington, IN, USA, 1999; (*b*) *Handbook of Chemistry and Physics*, Chemical Rubber Company, Cleveland, OH, USA, 52nd edn, 1971–1972, E108E122.

24 S. Piligkos, G. Rajaraman, M. Soler, N. Kirchner, J. van Slageren, R. Bircher, S. Parsons, H.-U. Güdel, J. Kortus, W. Wernsdorfer, G. Christou and E. K. Brechin, *J. Am. Chem. Soc.*, 2005, **127**, 5572.

25 G. Rajaraman, M. Murugesu, E. C. Sanudo, M. Soler, W. Wernsdorfer, M. Helliwell, C. Muryn, J. Raftery, S. J. Teat, G. Christou and E. K. Brechin, *J. Am. Chem. Soc.*, 2004, **126**, 15445.

26 D. Foguet-Albiol, T. A. O'Brien, W. Wernsdorfer, B. Moulton, M. J. Zaworotko, K. A. Abboud and G. Christou, *Angew. Chem., Int. Ed.*, 2005, **44**, 897.

27 G. Rajaraman, E. C. Sanudo, M. Helliwell, S. Piligkos, W. Wernsdorfer, G. Christou and E. K. Brechin, *Polyhedron*, 2005, **24**, 2450.

28 (*a*) R. W. Saalfrank, T. Nakajima, N. Mooren, A. Scheurer, H. Maid, F. Hampel, C. Trieflinger and J. Daub, *Eur. J. Inorg. Chem.*, 2005, 1149; (*b*) Th. C. Stamatatos, K. M. Poole, D. Foguet-Albiol, K. A. Abboud, T. A. O'Brien and G. Christou, *Inorg. Chem.*, 2008, **47**, 6593.

29 (*a*) A. Escuer and G. Aromi, *Eur. J. Inorg. Chem.*, 2006, 4721; (*b*) Th. C. Stamatatos, B. S. Luisi, B. Moulton and G. Christou, *Inorg. Chem.*, 2008, **47**, 1134; (*c*) Th. C. Stamatatos, K. A. Abboud, S. P. Perlepes and G. Christou, *Dalton Trans.*, 2007, 3861; (*d*) T. Taguchi, Th. C. Stamatatos, K. A. Abboud, C. M. Jones, T. A. O'Brien and G. Christou, *Inorg. Chem.*, 2008, **47**, 4095; (*e*) Th. C. Stamatatos and G. Christou, *Inorg. Chem.*, 2008, in press.

30 I. D. Brown and D. Altermatt, *Acta Crystallogr., Sect. B: Struct. Sci.*, 1985, **41**, 244; W. Liu and H. H. Thorp, *Inorg. Chem.*, 1993, **32**, 4102.

31 W. Quellette, A. V. Prosvirin, J. Valeich, K. R. Dunbar and J. Zubieta, *Inorg. Chem.*, 2007, **46**, 9067.

32 C. J. Matthews, L. K. Thompson, S. R. Parsons, Z. Xu, D. O. Miller and S. L. Heath, *Inorg. Chem.*, 2001, **40**, 4048.

33 S. Brooker, V. McKee and T. Metcalfe, *Inorg. Chim. Acta*, 1996, **246**, 171.

34 C. J. Matthews, Z. Xu, S. K. Mandal, L. K. Thompson, K. Biradha, K. Poirier and M. J. Zaworotko, *Chem. Commun.*, 1999, 347.

35 M. S. Lah and V. L. Pecoraro, *J. Am. Chem. Soc.*, 1989, **111**, 7258.

36 C. Dendrinou-Samara, A. N. Papadopoulos, D. A. Malamatari, A. Tarushi, C. P. Raptopoulou, A. Terzis, E. Samaras and D. P. Kessissoglou, *J. Inorg. Biochem.*, 2005, **99**, 864.

37 C.-I. Yang, W. Wernsdorfer, G.-H. Lee and H.-L. Tsai, *J. Am. Chem. Soc.*, 2007, **129**, 456.

38 T. Shiga and H. Oshio, *Polyhedron*, 2007, **26**, 1881.

39 C. P. Berlinguette, D. Vaughn, C. Canada-Vilalta, J. R. Galan-Mascaros and K. R. Dunbar, *Angew. Chem., Int. Ed.*, 2003, **42**, 1523.

40 R. A. Reynolds and D. Coucouvanis, *Inorg. Chem.*, 1998, **37**, 170.

41 D. V. Behere and S. Mitra, *Inorg. Chem.*, 1980, **19**, 1992; B. J. Kennedy and K. S. Murray, *Inorg. Chem.*, 1985, **24**, 1552, and references therein.

42 B. Albela, R. Carina, C. Policar, S. Poussereau, J. Cano, J. Guilhem, L. Tchertanov, G. Blondin, M. Delroisse and J.-J. Girerd, *Inorg. Chem.*, 1985, **24**, 4454; G. Aromi, J. Telser, A. Ozarowski, L.-C. Brunel, H.-M. Stoeckli-Evans and J. Krzystek, *Inorg. Chem.*, 2005, **44**, 187, and references therein.

43 J. Krzystek, J. Telser, M. J. Knapp, D. N. Hendrickson, G. Aromi, G. Christou, A. Angerhofer and L.-C. Brunel, *Appl. Magn. Reson.*, 2001, **23**, 571.

44 J. Limburg, J. S. Vrettos, R. H. Crabtree, G. W. Brudvig, J. C. de Paula, A. Hassan, A.-L. Barra, C. Duboc-Toia and M.-N. Collomb, *Inorg. Chem.*, 2001, **40**, 1698.

45 K. J. Kambe, *Phys. Soc. Jpn.*, 1950, **5**, 48.

46 E. C. Sañudo, W. Wernsdorfer, K. A. Abboud and G. Christou, *Inorg. Chem.*, 2004, **43**, 4137; C. Lampropoulos, M. Murugesu, K. A. Abboud and G. Christou, *Polyhedron*, 2007, **26**, 2129.

